Effect of reverse sodium flux and pH on ammoniacal nitrogen transport through biomimetic membranes

Kedwell, Katie Charlotte; Christensen, Morten Lykkegaard; Quist-Jensen, Cejna Anna; Jørgensen, Mads Koustrup

Published in:
Separation and Purification Technology

DOI (link to publication from Publisher):
10.1016/j.seppur.2019.02.001

Publication date:
2019

Document Version
Accepted author manuscript, peer reviewed version

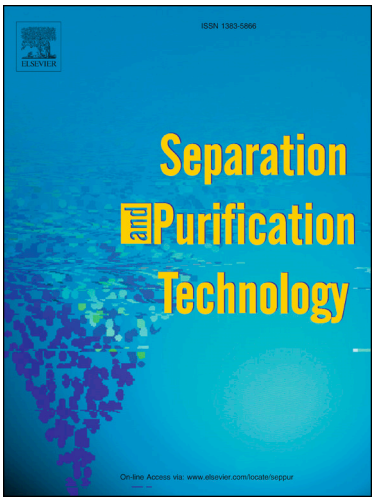

Effect of reverse sodium flux and pH on ammoniacal nitrogen transport through biomimetic membranes

Katie C. Kedwell, Morten L. Christensen, Cejna A. Quist-Jensen, Mads K. Jørgensen

PII: S1383-5866(18)34172-8
DOI: https://doi.org/10.1016/j.seppur.2019.02.001
Reference: SEPPUR 15311

To appear in: *Separation and Purification Technology*

Received Date: 27 November 2018
Revised Date: 1 February 2019
Accepted Date: 1 February 2019

Please cite this article as: K.C. Kedwell, M.L. Christensen, C.A. Quist-Jensen, M.K. Jørgensen, Effect of reverse sodium flux and pH on ammoniacal nitrogen transport through biomimetic membranes, *Separation and Purification Technology* (2019), doi: https://doi.org/10.1016/j.seppur.2019.02.001

Effect of reverse sodium flux and pH on ammoniacal nitrogen transport through biomimetic membranes

Katie C. Kedwell, Morten L. Christensen, Cejna A. Quist-Jensen, Mads K. Jørgensen*

Center for Membrane Technology, Department of Chemistry and Bioscience, Aalborg University, Fredrik Bajers Vej 7H, 9220 Aalborg Øst, Denmark

Abstract

Forward osmosis can be used to treat wastewater using seawater as the draw solution. This has been done for both water purification and nutrient concentration. However, the loss of ammoniacal nitrogen to the draw solution may be a key issue, reducing nutrient recovery and preventing the discharge of untreated seawater draw solution – a cost-saving strategy for the industrialisation of forward osmosis for wastewater treatment. In this study, forward ammoniacal nitrogen flux was studied using digester centrate from a wastewater treatment plant as the feed solution. The draw solution contained various NaCl concentrations in order to determine the effect of reverse sodium flux on forward ammoniacal nitrogen flux. The forward ammoniacal nitrogen flux was measured to be 1.5×10^{-6} – 8.0×10^{-5} mol m^{-2} s^{-1}, and increased with pH and sodium concentration in the draw solution. The forward ammonium flux increased with draw solution reverse salt flux below pH = 9, whereas it was unaffected by this flux above pH = 9. Therefore, the reverse flux of sodium ions facilitates the forward transport of ammonium ions at low pH. The transport of the positively charged ammonium was lower than that of the neutral ammonia due to its higher hydrodynamic radius.

Keywords: Forward osmosis; Aquaporin; Biomimetic membrane; Ammonia; Ammonium

1. Introduction

Reverse osmosis (RO) and more recently forward osmosis (FO) are both technologies used to produce clean water and can potentially be used for simultaneous water purification and nutrient concentration. RO is driven by the pressure drop across the membrane; in contrast, FO is driven by the difference in osmotic pressure across the membrane, so a high-osmotic-pressure draw solution is used to draw water from the feed solution to be treated [1]. Both RO and FO may also be used in treating both industrial and municipal wastewater. This is relevant both to water purification and nutrient recovery; for example, FO has been investigated for use in concentrating wastewater for subsequent phosphorus and ammonium recovery [2–5]. FO has a lower fouling propensity as it is not pressure driven [1,6], so it is preferable to pressure-driven processes (e.g., RO) when treating wastewater that contains various foulants. Therefore, many previous studies have considered the use of forward osmosis for phosphorus (P) recovery from wastewater and sludge.

Ammoniacal nitrogen transfer is also an important parameter in nutrient recovery from wastewater [3,7,8], as municipal wastewater often contains a high concentration of ammoniacal nitrogen (i.e., ammonia and ammonium). Thin-film composite (TFC) and cellulose triacetate (CTA) membranes have traditionally been used in concentrating wastewater using forward osmosis. However, the small molecular radius of ammonia [9] means that the rejection of ammoniacal nitrogen has been measured to be only 62–93.3% [10,11] for CTA membranes in the FO treatment of reject water [12], which is low compared with, for example, the >92% rejection of phosphate [3,12,13]. Ammoniacal nitrogen could cause eutrophication if it exceeds the effluent consents set for the wastewater treatment plant (WWTP) [14], and in drinking water, ammoniacal nitrogen exceeding 0.2 mg L^{-1} will cause odour and taste issues [15]. In addition, low rejection of ammoniacal nitrogen results in loss of potentially recoverable nutrients and contamination of the draw solution [16], which then may have to be treated before discharge [17]. Previous studies have achieved this by subjecting the draw solution to anammox treatment [18]. It is therefore necessary to determine whether rejection of ammoniacal nitrogen is sufficient if seawater draw solution is to be discharged without treatment, and to understand the mechanisms and parameters affecting ammoniacal nitrogen transport across the membrane.

Ammonia (NH_3) molecules are small and uncharged, allowing them to pass through a membrane more easily than charged ammonium (NH_4^+). The hydrodynamic radius is 330 pm for ammonium, versus 180 pm for ammonia (see Table S2 [19] in the Supplementary Information). Thus, the hydrodynamic radius of ammonium is comparable to the size of sodium and potassium ions [20], which are often found in seawater draw solution when using FO and which can increase the reverse salt flux from draw to feed. FO membranes usually consist of an ultra-thin active layer (>1 µm [1]), allowing high water flux and low reverse salt flux, supported by a porous support layer [21,22]. It has been suggested that FO has a lower rejection of ammoniacal nitrogen than does RO, as in FO, ammonium ions are transferred through the FO membrane with the counter-transport of sodium co-ions from the draw solution side of the membrane [23,24]. Diffusion of the uncharged ammonia form may occur, as the small size and the neutrality of the molecule enables it to permeate the membrane [23,24]. The transport is dependent on pH [2], due to the transition from charged ammonium to uncharged ammonia at around pH = 9.25.

Over the past decade, new RO and FO membranes have become available. One such type of membrane is biomimetic membranes, which utilise aquaporin protein channels. These display higher contaminant rejection than do TFC or CTA membranes, while maintaining a high water flux of 15.6 L m^{-2} h^{-1} (LMH) when using a 0.5 M NaCl draw solution [25]. These membranes differ considerably from TFC or CTA membranes, as the number of vesicles per area plays a key role in determining the water flux that the membrane can achieve. Biomimetic (aquaporin) membranes have been tested in both RO and FO modes. In RO mode, the membranes were found to have a NaCl rejection of 97.0–97.2% [26,27] using 5 bar pressure

[26] and a water recovery of 90% [27]. Schneider et al. (2018) found 96.95%, 95.87%, and 99.83% rejections of ammoniacal nitrogen, total nitrogen, and total phosphorus, respectively, i.e., higher than for CTA and TFC membranes [24].

Transport of ammoniacal nitrogen through the aquaporin channel is expected to be low, as aquaporin proteins are highly selective [28], but ammoniacal nitrogen may be transported via the TFC membrane or the vesicles of which the aquaporin membrane consists. There may be two mechanisms by which ammoniacal nitrogen moves across the membrane: convection induced by permeation drag and diffusion driven by a concentration gradient across the membrane (Eq. (1)) [29]:

$$J_{NH_3} = (1-\sigma)CJ_w + \omega\Delta C \quad (1)$$

In the above equation, σ is the reflection coefficient, C is concentration (mol m^{-3}), J_w is the permeate volume flux (m s^{-1}), ω is the solute permeability coefficient (m s^{-1}), and ΔC is the concentration difference (mol m^{-3}) across the membrane from feed to draw solution. Ammonium is positively charged, so transport is also influenced by the electrical field in the membrane [30]:

$$J_{NH_4^+} = -K_d D_i \frac{dc^m}{dx} - \frac{z_i c^m K_d D_i}{RT} F \frac{d\psi^m}{dx} + K_c c^m J_w \quad (2)$$

where K_d is the hindrance coefficient, D_i is the ion diffusion coefficient (m^2 s^{-1}), c^m is the concentration (mol m^{-3}), x is the axial coordinate (m), z_i is the charge number, R is the ideal gas constant (8.3143 J mol^{-1} K^{-1}), T is the temperature (K), F is Faraday's constant (96,487 C mol^{-1}), ψ^m is the electrical potential (V), and J_w is the permeate volume flux (m s^{-1}).

To ensure electroneutrality, ammonium can be exchanged with a cation moving from the draw to the feed solution or it can be co-transported from feed to draw with an anion, such as Cl^- (Fig. 1) [31]. However, Cl^- forward flux may not occur, as there is a higher concentration of chloride in draw than in feed. Instead, in the case of a high reverse salt flux, a lower reverse chloride salt flux relative to the sodium reverse salt flux may facilitate ammonium forward flux. It follows that ammonium transport may be affected by the composition of the feed, for example, the concentration of anions and cations and the salt type and concentration in the draw solution. This may affect the rejection of ammonium, and higher rejection can be expected in RO operations, in which no co-ions exist on the permeate side, than in FO, in which the salt concentration can be rather high on the draw side and reverse salt flux has been found to be an issue [32]. Salt rejection depends on the size and charge of the ions, as described by the following equation [33]:

$$\frac{c_i}{C_i} = \phi_i \, e^{\left(-\frac{z_i F}{RT}\Delta\psi_D\right)} \, e^{\left(\frac{-\Delta W_i}{kT}\right)} \quad (3)$$

where c_i is the concentration of ion i within the membrane (mol m^{-3}), C_i is the ionic solute bulk solution concentration (mol m^{-3}), φ_i is the steric partition coefficient, ΔW_i is the Born solvation energy barrier (J), and k is the Boltzmann constant (1.38066×10^{-23} J K^{-1}).

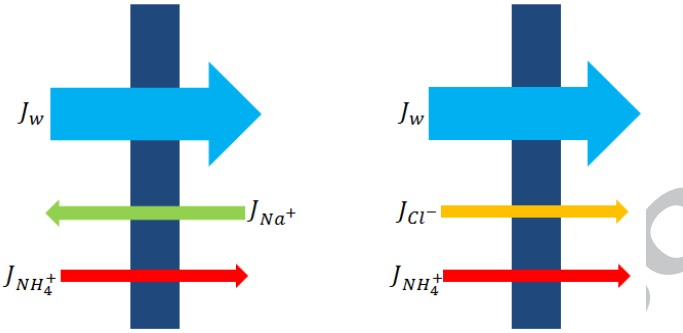

Fig. 1. Simplified diagram of ammonium transport methods; sodium and chloride ions have been used to illustrate counter- and co-transport due to their relatively small sizes (180 and 330 pm hydrated radius, respectively).

Reverse salt flux has been measured in several studies and is often measured to be < 4.75×10^{-5} mol m^{-2} s^{-1} [34–40], though some studies have reported reverse salt fluxes of up to 2.76×10^{-4} mol m^{-2} s^{-1} [41]. If the concentration of ammoniacal nitrogen in the permeate is the same as in the feed, no rejection is observed.

In this study, the mechanism of forward ammoniacal nitrogen transport across aquaporin biomimetic membranes is studied at varying pH levels and draw salt concentrations, inducing varying water fluxes, to evaluate the membrane for nutrient recovery from digester centrate and to describe the influence of pH and reverse sodium flux on forward ammoniacal nitrogen flux.

2. Materials and methods

2.1. Draw and feed solutions

Digester centrate was collected from Aaby WWTP (Aarhus, Denmark), an 84,000 Person equivalents (PE) municipal WWTW, using denitrification/nitrification and enhanced biological phosphorus removal (EBPR) treatment. At the plant, ferric chloride was added to control the concentration of total P, and excess EBPR sludge was pre-thickened and added to a mesophilic digester with a residence time of 20–22 days. This sludge was then dewatered in a decanter centrifuge and the digester centrate was collected for this study. The composition of digester centrate collected from Aaby WWTW can be found in Table 1.

The digester centrate was concentrated by means of forward osmosis using salt solutions of varying concentrations as the draw solutions. The draw solutions were seawater (equivalent to 0.599 M), 0.428 M and 0.770 M NaCl solutions (giving three measurements of water flux per investigated pH), and a NaCl solution with osmotic pressure equal to that of the feed solution.

Table 1
Digester centrate composition, pH, electrical conductivity, and osmotic pressure.

Parameter	Digester centrate (feed solution)
Ortho-P (mM)	1.7 ± 0.3
Total P (mM)	9.4 ± 0.3
Ammoniacal nitrogen (mM)	122 ± 5
Mg^{+} (mM)	0.04 ± 0.0009
Ca^{+} (mM)	1.1 ± 0.05
Na^{+} (mM)	3.7 ± 1.0
Cl^{-} (mM)	209 ± 51
pH	8.0 ± 0.2
Electrical conductivity (mS cm^{-1})	13.189 ± 0.007
Osmotic pressure (bar)	1.8 ± 0.3

2.2. FO setup and operation

A bench-scale FO setup (Fig. 2) was used to investigate the rejection of ammoniacal nitrogen and phosphate. Experiments were conducted using a membrane cell (Sepa FO cell; Sterlitech, Kent, WA, USA) with 140 cm^2 of active membrane area. Experiments were conducted with the membrane's active layer facing the feed solution to minimise fouling [42]. For the first 30 s of the experiments, the crossflow velocity (CFV) was 0.17 m s^{-1} to remove air from the system, after which the draw and feed solutions were circulated at 0.09 m s^{-1} by a peristaltic pump (Model: HV-07528-10; Masterflex, Vernon Hills, IL, USA). The CFV was controlled by the volumetric crossflow (L s^{-1}) and was calculated by dividing the crossflow by the cross-sectional area of the cell feed or draw chamber. All experiments were conducted at room temperature (20 ± 2.5°C) and the solutions were circulated between the membrane module and solution containers, with the draw solution container being placed on a balance. Data on the weight of the draw solution were acquired to determine the permeate flow and from that the flux. Water flux, J_w (m s^{-1}), was calculated using the change in mass, Δm (kg), of the draw solution per unit of time, Δt (s), and membrane area, A_m (m^2), as per Eq. 4. The density of water, ρ (kg m^{-3}), was set to 1000 kg m^{-3}.

$$J_w = \frac{\Delta m}{\rho A_m \Delta t} \quad (4)$$

The flux values are presented in L m^{-2} h^{-1} (LMH).

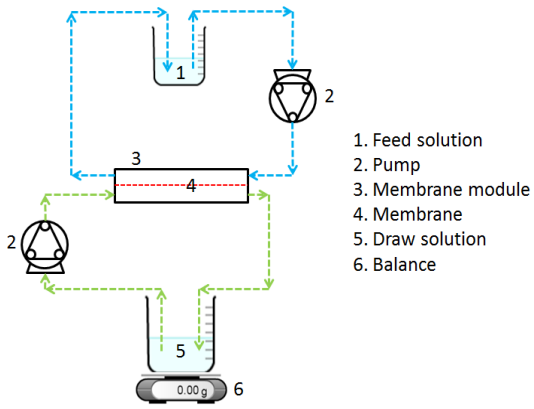

Fig. 2. Schematic of the bench-scale setup.

Biomimetic flat-sheet membranes (Aquaporin A/S, Kongens Lyngby, Denmark) were used for all experiments. The membranes consisted of a polyethersulfone porous support layer coated with a polyamide (TFC) active layer containing vesicles with aquaporin proteins. The vesicles house multiple aquaporin channels, allowing for the fast and selective transport of water through the membrane [26]. The membranes were 110 µm ± 15 µm thick and had a pH range of 2–11. Before use, the membranes were soaked in deionised water for 24 h to activate them and remove particulates and compounds left on the surface by the manufacturing process.

Initial experiments were conducted for one hour to determine the water permeability. For these experiments, the feed solution was deionised water and the draw solutions were 0.428, 0.513, 0.598, 0.684, and 0.770 M NaCl solutions (with 20.8, 25.0, 29.2, 33.3, and 37.5 bar osmotic pressures, respectively). The water permeability, A (LMH bar^{-1}) was calculated from Eq. (5):

$$A = \frac{J_w}{\Delta \pi} \quad (5)$$

In the experiments to study ammoniacal nitrogen transport, digester centrate was used as the feed solution and the experiments were operated at different pH levels. The pH was measured using a MeterLab PHM220 pH meter (Hach, Loveland, CO, USA) and was adjusted using 10% v/v H_2SO_4 and 1 M NaOH. The experiments were conducted at pH 5, 7, 8, 9.25, and 10 to investigate the influence of solute charge on the transport mechanism through the membrane. To investigate the influence of reverse sodium diffusion on forward ammoniacal nitrogen transport, all the above experiments were conducted with different draw solutions, i.e., seawater and 0.428 and 0.770 M NaCl solutions. In addition, a NaCl draw solution was used

with an electrical conductivity equal to that of the digester centrate, in order to have no water flux and a negligible gradient in sodium concentration, i.e., so that ammoniacal nitrogen transport was controlled by diffusion rather than convection. Every 0.5 h, 15-mL samples of feed and draw solutions were taken for chemical analysis. The filtration time was 4 h, during which the weight of the draw solution was recorded every 10 min for the first hour and every 0.5 h thereafter. For each experiment, 1 L of feed and 2 L of draw solutions were used. A larger volume of draw solution than feed solution was used to reduce the draw dilution, which was further reduced by the short filtration time of 4 h.

The osmotic pressures of the feed solution and seawater draw solution were determined through the water activity, a_w, of the samples [2], measured using an AquaLab water activity meter (Meter Group, Pullman, WA, USA) at 25℃. The osmotic pressure was then calculated from the water activity using Eq. (6):

$$\pi = -\left(\frac{RT}{V_m}\right)\ln(a_w) \quad (6)$$

where R is the gas constant (0.0831 L bar mol^{-1} K^{-1}), T is the temperature (K), and V_m is the partial molar volume of water (0.018 L mol^{-1}). It was assumed that NaCl draw solution osmotic pressures could be determined using the Van 't Hoff equation (Eq. 7), which is for ideal, dilute solutions:

$$\pi = iMRT \quad (7)$$

where M is the molarity of salt (M) and i is the Van 't Hoff Factor, a measure of the number of ions a solute will form when dissolved in water. Since NaCl in seawater is fully dissociated, i equals 2.

2.3. Analysis of solute transport

Ammoniacal nitrogen and sodium concentrations were measured in all samples. Ammoniacal nitrogen was measured in feed and draw solution samples using a spectrophotometric method according to Danish standards [43]. Sodium was measured in feed and draw solution samples using atomic absorption spectroscopy. The concentration of chloride ions was also measured in feed and draw solutions. This was done by measuring the mV potential of diluted samples (diluted by a factor of 100–400 in 0.1 M KNO_3) with a chloride ion–selective electrode (Model: ISE25Cl; Radiometer Analytical, Lyon, France), and calculating the chloride concentration from a standard curve ranging from 0.1 to 100 mM chloride ions. The remaining water parameters were measured using standard methods [44].

Solute flux, J_s (mol m^{-2} s^{-1}), was calculated using the following equation:

$$J_s = \frac{C_{s,F,initial} V_{initial} - C_{s,F,final} V_{final}}{A_m \times t} \quad (8)$$

where $C_{s,F,initial}$ and $C_{s,F,final}$ (mol L^{-1}) are the initial and final feed solute concentrations and $V_{initial}$ and V_{final} (L) are the initial and final volumes, respectively. It should be noted that a reverse flux of solutes, i.e., from draw to feed solution, will give a negative solute flux; such fluxes will be called reverse fluxes of solutes with positive values.

The specific forward solute flux of ammoniacal nitrogen in the permeate, C_N* (M), is given as the ratio between the forward ammoniacal nitrogen flux, J_N (mol m^{-2} s^{-1}), and the water flux (m s^{-1}):

$$C_N^* = \frac{J_{Ns}}{J_w} \quad (9)$$

This corresponds to the concentration of ammoniacal nitrogen in the water permeating the membrane (permeate); it is not the concentration in the draw solution, which will be lower due to dilution of the ammoniacal nitrogen–rich water permeating the membrane and will increase throughout the FO process. C_N* can then be used in calculating the ammoniacal nitrogen rejection.

There are several methods for calculating rejection. The first method uses Eq. (10) [12] [45], where C_D and C_F are the draw and feed ammoniacal nitrogen concentrations (M), respectively:

$$R = \left(1 - \frac{C_D}{C_F}\right) \times 100\% \quad (10)$$

However, this equation does not make sense for the experimental design underlying this study, as the draw will continuously dilute the ammoniacal nitrogen transported from the feed. Simply using the mass of solute in the feed and draw solutions will also give a false value: it will be time dependent, as a steady-state concentration will not be reached. Hence, in the batch experiments, a steady-state concentration will not be reached and the rejection calculated from Eq. (10) will depend on the draw volume, time, and the concentration factor of the feed. Instead, the rejection can be found by calculating the apparent concentration in the water permeating the membrane. This gives a rejection comparable to that of pressure-driven membrane filtration, which is independent of, for example, the dilution effects of the draw solution. This is done by combining Eq. (9) and Eq. (10) to form Eq. (11), here with C_F expressed in mol m^{-3} and J_w in m s^{-1}:

$$R = \left(1 - \frac{J_s}{J_w C_F}\right) \times 100\% \quad (11)$$

Another way of characterising the membrane's ability to transport or reject the solutes is through the solute flux. The flux of ammonia is described by Eq. (1), whereas we propose a simplified version of Eq. (2) to

calculate the flux of ammonium specific to the parameters relevant to this study, i.e., transport based on the exchange of sodium ions, and pH-dependent transport governed by diffusion:

$$J_{NH_4^+} = k'(pH, \Delta c_{NH_4^+}) + k''(pH, \Delta c_{NH_4^+}) c_{Na^+,D} \quad (12)$$

where $c_{Na^+,D}$ is the concentration of sodium ions in the draw solution (M), *k'* is the flux of ammonium with co-transport of an anion (mol m^{-2} s^{-1}), $\Delta c_{NH_4^+}$ is the concentration gradient of ammonium across the membrane (from feed to draw solution) (M), *k''* is the transport of ammonium due to the counter-transport of sodium ions from the draw solution (m s^{-1}), and $C_{Na+,D}$ is the concentration of sodium ions in the draw solution (mol m^{-3}). In other words, the first term of the equation is the transport of ammonium from feed to draw with a counter-ion, whereas the second term is the counter-transport of sodium (co-ion), which depends on sodium flux and thereby on the sodium concentration in the draw solution. Both *k'* and *k''* are functions of the pH, which affects the charge of ammoniacal nitrogen and other ions in the feed. It is assumed that the transport of ammonium due to the co-transport of anions and counter-transport of cations is additive in order to maintain electroneutrality between the feed and draw solutions.

The total forward flux of ammoniacal nitrogen is given as the sum of the forward ammonia and ammonium fluxes. The sodium ion flux (mol m^{-2} s^{-1}) is a reverse transport from the draw to feed solution (i.e., a negative transport from feed to draw); it is assumed to be proportional to the concentration of salt in the draw solution, as the initial concentration of sodium ions in the feed is negligible and does not contribute to the concentration gradient. The reverse sodium ion flux depends on the sodium concentration in the draw solution, as described by the following expression:

$$J_{Na^+} = k''' c_{Na^+,D} \quad (13)$$

where *k'''* is the sodium ion permeability (m s^{-1}). Combining Eq. (12) and (13) gives Eq. (14):

$$J_{Na^+} = k''' c_{Na^+,D} \quad (14)$$

where λ is *k''/k'''*, i.e., the fraction of the reverse sodium ion transport linked to the ammonium transport. The fraction of ammoniacal nitrogen present as ammonium ($\alpha_{NH_4^+}$) was calculated from Eq. (15):

$$\alpha_{NH_4^+} = \frac{1}{1+\frac{K_a}{[H^+]}} \quad (15)$$

where $[H^+]$ is the concentration of hydrated protons and K_a is the dissociation constant, which is 5.62×10^{-10} M for ammoniacal nitrogen (calculated from $pK_a = 9.25$).

3. Results and discussion

3.1. Water permeability

The water flux for biomimetic membranes was determined for both deionised water and digester centrate feed solution. In Fig. 3, the measured water fluxes (average values over 4 h with standard deviations) are plotted against the osmotic pressure differences (five for deionised water feeds and fifteen for digester centrate feeds at five pH levels and for three draw solutions, i.e., seawater and 0.428 and 0.770 M NaCl). There was negligible water permeation for experiments with varying equal osmotic pressures of feed and draw solutions (not shown in Fig. 3). The plot shows higher water fluxes for deionised water feed solutions than for digester centrate feed solutions, indicating that the external concentration polarization of solutes and fouling on the feed side reduce the water flux. The water flux increases with $\Delta\pi$ for both deionised water and digester centrate feed solutions, corresponding to the higher driving force provided by a higher salt concentration in the draw. Water flux has been measured at different pH levels, but no correlation between pH and water flux was found for any of the draw solutions used (data not shown). Conversely, water permeability in experiments with deionised water feed was calculated using Eq. 5, giving a decline in permeability from 0.25 to 0.20 LMH bar^{-1} with increasing osmotic pressure difference. This can be explained by concentration polarization reducing the effective permeability of the membrane or by membrane fouling. The average water permeability when using digester centrate feed solution is 0.083 LMH bar^{-1}, which, as expected, is lower than that of the deionised water feed. This is explained by further concentration polarization caused by the feed solutes. The average water flux was 5.2 and 2.0 LMH for the deionised water and digester centrate feed solutions, respectively. Previous studies using similar biomimetic aquaporin membranes found a water flux of 1.5 LMH when using a 0.428 M NaCl draw solution and a deionised water feed solution; furthermore, a water flux of 5.5 LMH was not achieved until a draw solution of 1.711 M NaCl was used [4]. This corresponds to water permeabilities of 0.072 and 0.062 LMH bar^{-1}, respectively, i.e., 30% of the deionised water permeability measured here. However, the water permeability for the aquaporin membrane is lower than, for example, that of commercially available TFC membranes, whose permeability was measured to be 0.90 and 0.27 LMH bar^{-1} for deionised water and digester centrate feed solution, respectively [2]. CTA membranes similar to the biomimetic membrane used here have been found to be capable of achieving a water permeability of 0.21 LMH bar^{-1} when using a 1.711 M draw solution and a deionised water feed solution [1]. An example of water recovery over time can be found in Fig. S1 in the Supplementary Information.

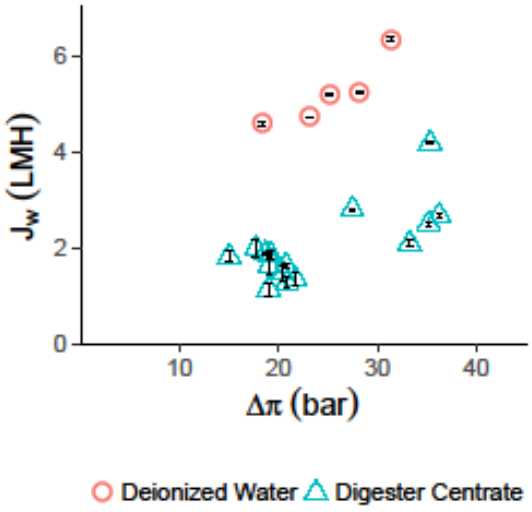

Fig. 3. Water flux using deionised water and digester centrate feed solution versus the difference in osmotic pressure across the membrane.

3.2. Transport mechanism for ammoniacal nitrogen

In addition to varying pH, the draw solution osmotic pressure was changed to induce different water fluxes, as doing so can indicate how both pH (affecting diffusive transport) and draw solution NaCl concentration (facilitating reverse ion transport) affect the transport mechanism for ammoniacal nitrogen. An example of feed solution concentrations of ammonium, chloride, and phosphate over the experimental period can be found in Fig. S1 in the Supplementary Information.

Fig. 4a shows the concentration of ammoniacal nitrogen in the feed solution and the apparent permeate ammoniacal nitrogen concentration (C_N*, calculated from the ratio between the forward ammoniacal nitrogen flux and the water flux, Eq. 9) at varying pH levels. The figure shows that C_N* increased with pH, meaning that there is a higher concentration in the water permeating the membrane. This increasing permeation of ammoniacal nitrogen is explained by increasing feed solution concentrations of ammonia relative to ammonium at higher pH. Therefore, the apparent rejection of ammoniacal nitrogen increased with decreasing pH. The apparent concentration of ammoniacal nitrogen in permeate was used to calculate the rejection using Eq. 11; the rejection is plotted against pH in Fig. 4b, along with the rejection calculated just from the feed and draw solution concentrations measured at the end of the experiments (according to Eq. (10)). Both ways of calculating rejections show decreasing values as a function of pH, but whereas the rejection calculated from Eq. (10) is above 94%, the rejection calculated from Eq. (11) is significantly lower, ranging from 35% (pH = 5) to –11% (pH = 10). The declining rejection with increasing pH is explained by

the higher prevalence of ammonia, whereas the lower rejection calculated by Eq. (11) is explained by it not being affected by the dilution of the solute transported through the membrane as it reaches the draw solution, as in the method underlying Eq. (10). Hence, Eq. (10) gives a falsely high rejection, as it is dependent on the draw solution volume to solute flux and on the concentration factor of the feed (i.e., how long the batch experiment runs). Instead, Eq. (11) describes the membrane's ability to reject the solute, but does not describe the concentration in the draw. Instead, the solute flux may be determined to characterise the membrane's ability to reject solutes.

Forward ammoniacal nitrogen fluxes ranged from 1.5×10^{-6} to 8.0×10^{-5} mol m^{-2} s^{-1}, with higher ammoniacal nitrogen fluxes at higher pH, in accordance with the lower rejections. These ammoniacal nitrogen fluxes are significantly lower than, for example, the ammoniacal nitrogen fluxes reported in the literature (e.g., ammoniacal nitrogen fluxes calculated by Soler-Cabezas et al. [4] using polyamide TFC membranes are in the range of $9.0 \times 10^{-4} – 1.1 \times 10^{-3}$ mol m^{-2} s^{-1}). CTA membranes were used in a second study, in which forward ammonium fluxes of 2.4×10^{-4} mol m^{-2} s^{-1} were observed for a concentration gradient of approximately 2000 mM [32]. A study using aquaporin membranes reported values corresponding to a forward ammoniacal nitrogen flux of approximately 1.2×10^{-4} mol m^{-2} s^{-1}; again, the concentration gradient of ammonium was significantly higher than in the current study at approximately 13–331 mM, versus 91 mM [48].

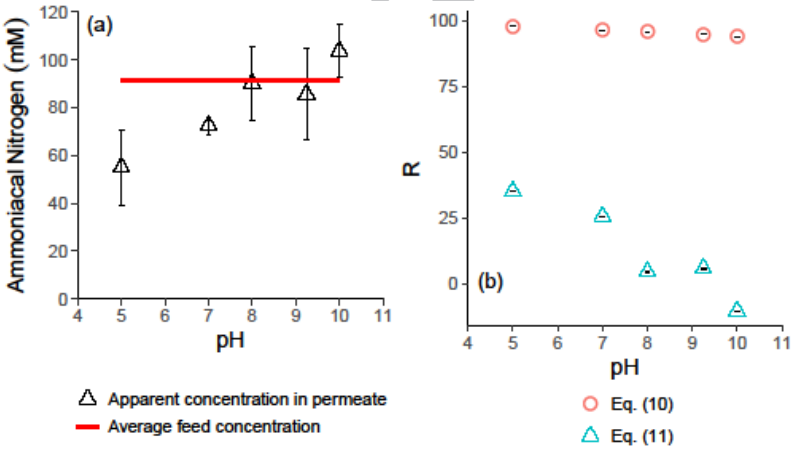

Fig. 4. (a) Apparent permeate ammoniacal nitrogen concentration relative to the feed concentration of digester centrate adjusted to different pH values, and (b) rejections as a function of pH calculated from the draw and feed solution concentrations (Eq. (10)) and from apparent permeate and feed concentrations (Eq. (11)), respectively.

For sodium, it was observed that higher draw solution NaCl concentrations resulted in higher reverse fluxes of sodium due to higher concentration gradients (data not shown). From linear regressions of forward ammoniacal nitrogen flux as a function of sodium flux, the slope of the forward ammoniacal nitrogen flux versus sodium flux was calculated for each pH, corresponding to λ in Eq. 14 (see Table S1 in the

Supplementary Information). These results are plotted against pH in Fig. 5a, together with the fraction of ammoniacal nitrogen present as ammonium at the given pH value (red line). Fig. 5a shows a higher dependency of sodium transport on ammoniacal nitrogen transport at low pH; this can be explained by the high reverse sodium flux enabling the forward transport of charged ammonium. As pH increases, the ammonia to ammonium ratio increases, i.e., because ammonia is uncharged, ammoniacal nitrogen transport becomes independent of the counter-transport of sodium ions, in accordance with the lack of a relationship between forward ammoniacal nitrogen flux and reverse sodium flux at high pH. Instead, uncharged ammonia has fewer electrostatic interactions with the membrane surface and a lower hydrodynamic radius, resulting in a constant high flux of ammonia driven by the ammonia concentration gradient across the membrane (Eq. (1)). The ammonia concentration gradient of 92 ± 15 mM was not varied in this study, though the higher draw solution osmotic pressures induced higher permeate fluxes (Fig. 3). Notably, the higher permeate fluxes at high pH (when ammonia was present) did not affect the forward ammoniacal nitrogen flux, i.e., the convective transport proposed in Eq. (1) is negligible and ammonia transport is only affected by a gradient in concentration. This was observed, as there is a lack of dependency between ammoniacal nitrogen and sodium fluxes at high pH, i.e. $\lambda \approx 0$. To support this statement, the forward ammoniacal nitrogen fluxes in experiments with no permeate flux (i.e., no convection, as the osmotic pressures of the feed equalled those of the draw solutions) are plotted against pH in Fig. 5b. The graph shows increasing diffusion with pH, i.e., when the amount of ammonia relative to ammonium increased, corresponding to the mechanism of ammonia transfer being diffusion at higher pH, as the ammonia molecule is small and uncharged (i.e., the diffusive ammonia transport equals the overall forward flux, meaning that no convective transport was observed).

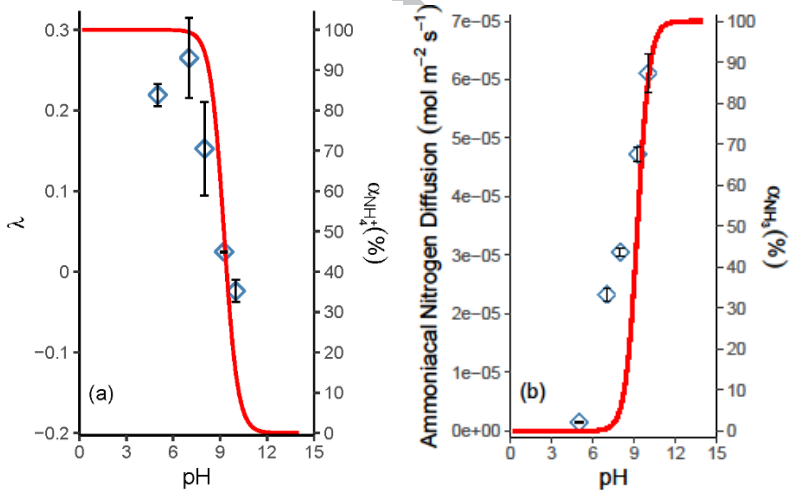

Fig. 5. (a) λ and fraction of ammoniacal nitrogen present as ammonium plotted as a function of pH, and (b) ammoniacal nitrogen diffusion and fraction of ammoniacal nitrogen present as ammonia plotted against pH.

The chloride flux was calculated from the rate of increase in chloride content in feed solutions throughout the FO experiments, and there was a correlation between reverse chloride and reverse sodium ion fluxes. Fig. 6

shows the ratio between reverse chloride and reverse sodium ion fluxes at varying pH levels found from the slope of linear regressions between the reverse chloride and reverse sodium fluxes. As seen in the figure, there is a decreasing correlation between the two fluxes with increasing pH. At pH 9 and 10 $\lambda_{Cl/Na}$, the correlation is around 1; therefore, the sodium and chloride reverse fluxes equal one another and are not involved in ammoniacal nitrogen transport at high pH levels, at which ammoniacal nitrogen is uncharged ammonia. Hence, chloride also acts as a counter-ion to sodium, enabling sodium transport. However, at low pH, the flux of chloride ions was significantly higher than the reverse flux of sodium or forward ammonium flux. This suggests that forward ammonium flux is not directly driven by forward chloride flux, as proposed in Fig. 1. In addition, other ions are also involved in the ionic exchange across the membrane, either positive from the draw solution or negative from the feed solution.

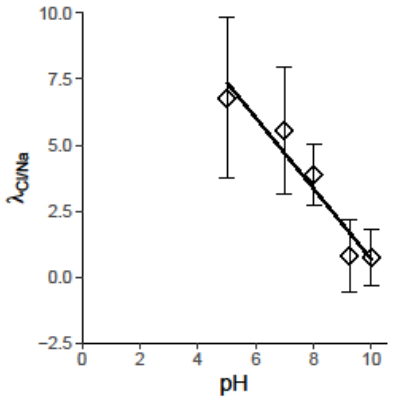

Fig. 6. Ratio between reverse chloride and reverse sodium fluxes at varying pH levels.

Ammonia has a smaller radius than the ions (Table S2 in Supplementary information), hence, it will permeate the membrane more easily, explaining the high diffusivity at high pH (Fig. 5b). However, sodium also has a relatively low diffusivity but is present in high concentrations resulting in a high reverse sodium flux to facilitate forward ammonium flux. Chloride and potassium ions both have relatively low hydrated radii and high diffusivities, so these are expected to be able to facilitate the transport of ammonium by chloride co-transport or potassium counter-transport. From the forward ammoniacal nitrogen to reverse sodium flux ratios (λ) in Fig. 5(a), it is observed that the forward ammonium flux at pH 5–8 was only 26.5–15.2% of the reverse sodium flux, i.e., more sodium ions than ammonium ions are moving in the opposite direction. This is supported by calculating *k'* from Eq. 14, which expresses the forward ammonium flux caused by transfer with a co-/counter-ion other than sodium. This was calculated for pH 5 and 7, as >99.4% of ammoniacal nitrogen is present as ammonium at these levels. At pH 5 and 7, *k'* was 5.89×10^{-6} and 1.44×10^{-5} mol m^{-2} s^{-1}, respectively, which are large fluxes compared with the average ammoniacal nitrogen fluxes at pH 5 and 7, which 2.41×10^{-5} mol m^{-2} s^{-1} and 3.81×10^{-5} mol m^{-2} s^{-1}, respectively.

Other ions must therefore be involved in the exchange of ions; for example, chloride may be transferred from the feed to draw solutions to facilitate ammonium ion transport. However, the ratio between the forward ammoniacal nitrogen flux and the reverse chloride ion flux at varying pH levels (Fig. S2 in the Supplementary Information) indicates a very small proportion of forward ammonium flux relative to chloride flux, and in addition, the chloride flux from the feed to draw solutions is negative, meaning that chloride ions move from draw to feed due to the high concentration gradient. This suggests that the main mechanism of ammonium transport from the feed to draw solutions in Fig. 1 is by exchange with sodium ions from the draw rather than by transport with chloride ions from the feed. Although sodium fluxes were higher than forward ammoniacal nitrogen fluxes, ammonium permeability ($2.88 \times 10^{-7} \pm 1.86 \times 10^{-7}$ m s^{-1} at pH = 5) and ammonia permeability ($6.91 \times 10^{-7} \pm 1.43 \times 10^{-7}$ m s^{-1} at pH = 10) were higher than the average sodium permeability ($1.07 \times 10^{-7} \pm 2.42 \times 10^{-7}$ m s^{-1}) by a factor of 2.7 to 6.4, possibly because of the higher diffusivity of ammoniacal nitrogen (Table S2 in the Supplementary Information) or because the internal concentration polarization on the draw side of the membrane reduced the sodium permeability. The present results suggest that the reverse transport of ions and pH significantly influence the rejection of ammoniacal nitrogen. At high pH, uncharged ammonia can diffuse through the membrane, whereas at low pH, the transport of ammonium depends on the counter-transport of cations or the co-transport of anions. The FO membrane rejection of ions is often tested in RO mode (i.e., by high pressure filtration of an ionic solution), in which there is no counter-transport of ions from the solute-free permeate. This may lead to a higher rejection of ions than in FO mode, in which the draw solutions typically contain ions in high concentrations to facilitate reverse ionic transport and to achieve electroneutrality. In addition, given that the concentration of NaCl in an FO draw solution is far greater than the concentration of ammonia in the feed solution, even a small percentage of the initial NaCl concentration could facilitate the transport of a larger percentage of ammonium ions, since their concentration is significantly lower. For a sustainable FO treatment to recover nutrients from digester centrate, it is essential that only a small amount of ammoniacal nitrogen is lost by diffusion to the FO draw solution. Based on the present results, it is suggested that operating at pH < 8 and with draw solutions comprising larger ions having lower diffusivities and higher hydrodynamic radii (or simply uncharged molecules such as glucose) will result in the optimal rejection of ammoniacal nitrogen for nutrient recovery.

Due to the low rejection of ammoniacal nitrogen, there is potential for high concentrations of ammoniacal nitrogen in the draw solution, depending on the feed concentration factor and on draw solution replacement. The ammoniacal nitrogen concentration may exceed the threshold limit for discharge to the sea, if a seawater draw solution is used. This would call for further treatment of the diluted draw solution before discharge or for membranes that reject more ammoniacal nitrogen. Alternatively, a draw solution with a low reverse salt flux may be used, to prevent the transport of ammonium ions.

4. Conclusion

The transport of ammoniacal nitrogen through FO membranes was studied during the concentration of digester centrate. Ammoniacal nitrogen diffusion increased with pH from 1.5×10^{-6} mol m^{-2} s^{-1} at pH 5 to 6.1×10^{-5} mol m^{-2} s^{-1} at pH 10. At low pH, where ammoniacal nitrogen is present as charged ammonium, the forward ammoniacal nitrogen flux increased with the reverse sodium flux, as reverse sodium transport helped ammonium transport to remain electroneutral, and the forward ammonium flux equalled 22% of the reverse sodium flux at pH 5. At pH 10, the reverse sodium flux had no effect on the forward ammoniacal nitrogen flux, as ammoniacal nitrogen was present as ammonia. Ammonia had a higher permeability through the biomimetic membranes than did ammonium. The present results suggest that ammoniacal nitrogen transport through forward osmosis membranes can be reduced by operating at pH below 9 and by selecting draw solutes with low reverse salt flux or with no charge to facilitate ammonium transport.

Acknowledgements

Innovation Fund Denmark is acknowledged for funding this research through the RecoverP project (Grant Number: 4106-00014B). Aaby WWTP is acknowledged for providing the digester centrate used in this study. Thanks are expressed to Lisbeth Wybrandt, Kamilla Agnethe Smith Hansen, and Henriette Casper Jensen for analysing the samples.

References

[1] T. Cath, A. Childress, M. Elimelech, Forward osmosis: Principles, applications, and recent developments, J. Memb. Sci. 281 (2006) 70–87. doi:10.1016/j.memsci.2006.05.048.

[2] K.C. Kedwell, C.A. Quist-Jensen, G. Giannakakis, M.L. Christensen, Forward osmosis with high-performing TFC membranes for concentration of digester centrate prior to phosphorus recovery, Sep. Purif. Technol. 197 (2018) 449–456. doi:10.1016/j.seppur.2018.01.034.

[3] A.J. Ansari, F.I. Hai, W.E. Price, L.D. Nghiem, Phosphorus recovery from digested sludge centrate using seawater-driven forward osmosis, Sep. Purif. Technol. 163 (2016) 1–7. doi:10.1016/j.seppur.2016.02.031.

[4] J.L. Soler-Cabezas, J.A. Mendoza-Roca, M.C. Vincent-Vela, M.J. Luján-Facundo, L. Pastor-Alcañiz, Simultaneous concentration of nutrients from anaerobically digested sludge centrate and pre-treatment of industrial effluents by forward osmosis, Sep. Purif. Technol. 193 (2018) 289–296. doi:10.1016/J.SEPPUR.2017.10.058.

[5] L. Huang, D.-J. Lee, J.-Y. Lai, Forward osmosis membrane bioreactor for wastewater treatment with phosphorus recovery, Bioresour. Technol. 198 (2015) 418–423. doi:10.1016/J.BIORTECH.2015.09.045.

[6] A. Achilli, T.Y. Cath, E.A. Marchand, A.E. Childress, The forward osmosis membrane bioreactor: A low fouling alternative to MBR processes, Desalination. 238 (2009) 10–21. doi:10.1016/j.desal.2008.02.022.

[7] S. Phuntsho, H.K. Shon, T. Majeed, I. El Saliby, S. Vigneswaran, J. Kandasamy, S. Hong, S. Lee, Blended Fertilizers as Draw Solutions for Fertilizer-Drawn Forward Osmosis Desalination, Environ. Sci. Technol. 46 (2012) 4567–4575. doi:10.1021/es300002w.

[8] J. Korenak, S. Basu, M. Balakrishnan, C. Hélix-Nielsen, I. Petrinic, Forward Osmosis in Wastewater Treatment Processes, Acta Chim. Slov. (2017) 83–94. doi:10.17344/acsi.2016.2852.

[9] S.A. Solin, Y.B. Fan, X.W. Qian, Ion size effects in alkali-ammonia ternary graphite intercalation compounds, Synth. Met. 12 (1985) 181–186. doi:10.1016/0379-6779(85)90107-9.

[10] Y. Gao, Z. Fang, P. Liang, X. Huang, Direct concentration of municipal sewage by forward osmosis and membrane fouling behavior, Bioresour. Technol. 247 (2018) 730–735. doi:10.1016/J.BIORTECH.2017.09.145.

[11] L. Chen, Y. Gu, C. Cao, J. Zhang, J.-W. Ng, C. Tang, Performance of a submerged anaerobic membrane bioreactor with forward osmosis membrane for low-strength wastewater treatment, Water Res. 50 (2014) 114–123. doi:10.1016/J.WATRES.2013.12.009.

[12] R.W. Holloway, A.E. Childress, K.E. Dennett, T.Y. Cath, Forward osmosis for concentration of anaerobic digester centrate, Water Res. 41 (2007) 4005–4014. doi:10.1016/j.watres.2007.05.054.

[13] N.C. Nguyen, S.S. Chen, H.Y. Yang, N.T. Hau, Application of forward osmosis on dewatering of high nutrient sludge, Bioresour. Technol. 132 (2013) 224–229. doi:10.1016/j.biortech.2013.01.028.

[14] D.J. Conley, H.W. Paerl, R.W. Howarth, D.F. Boesch, S.P. Seitzinger, K.E. Havens, C. Lancelot, G.E. Likens, Controlling Eutrophication: Nitrogen and Phosphorus, Sci. Mag. (2009) 1014–1015.

[15] W. Kühn, Oxidation Techniques in Drinking Water Treatment: Papers Presented at the Conference Held in Karlsruhe, Federal Republic of Germany, September 11-13, 1978, 1979.

[16] A.J. Ansari, F.I. Hai, W.E. Price, J.E. Drewes, L.D. Nghiem, Forward osmosis as a platform for resource recovery from municipal wastewater - A critical assessment of the literature, J. Memb. Sci.

(2017). doi:10.1016/j.memsci.2017.01.054.

[17] J.C. Ortega-Bravo, G. Ruiz-Filippi, A. Donoso-Bravo, I.E. Reyes-Caniupán, D. Jeison, Forward osmosis: Evaluation thin-film-composite membrane for municipal sewage concentration, Chem. Eng. J. 306 (2016) 531–537. doi:10.1016/j.cej.2016.07.085.

[18] X. Li, Y. Lu, Z. He, Removal of reverse-fluxed ammonium by anammox in a forward osmosis system using ammonium bicarbonate as a draw solute, J. Memb. Sci. 495 (2015) 424–430. doi:10.1016/J.MEMSCI.2015.08.038.

[19] I.D. Weiner, J.W. Verlander, Renal Ammonia Metabolism and Transport, Compr. Physiol. 3 (2013) 201–220. doi:10.1002/cphy.c120010.

[20] C.R. Company., CRC handbook of chemistry and physics., CRC Press, Boca Raton, 1993.

[21] L.-F. Fang, L. Cheng, S. Jeon, S.-Y. Wang, T. Takahashi, H. Matsuyama, Effect of the supporting layer structures on antifouling properties of forward osmosis membranes in AL-DS mode, J. Memb. Sci. (2018). doi:10.1016/j.memsci.2018.02.028.

[22] R. Wang, L. Shi, C.Y. Tang, S. Chou, C. Qiu, A.G. Fane, Characterization of novel forward osmosis hollow fiber membranes, J. Memb. Sci. 355 (2010) 158–167. doi:10.1016/J.MEMSCI.2010.03.017.

[23] J.T. Arena, S.S. Manickam, K.K. Reimund, B.D. Freeman, J.R. McCutcheon, Solute and water transport in forward osmosis using polydopamine modified thin film composite membranes, Desalination. 343 (2014) 8–16. doi:10.1016/J.DESAL.2014.01.009.

[24] C. Schneider, R.S. Rajmohan, A. Zarebska, P. Tsapekos, C. Hélix-Nielsen, Treating anaerobic effluents using forward osmosis for combined water purification and biogas production, Sci. Total Environ. 647 (2019) 1021–1030. doi:10.1016/J.SCITOTENV.2018.08.036.

[25] W. Luo, M. Xie, X. Song, W. Guo, H.H. Ngo, J.L. Zhou, L.D. Nghiem, Biomimetic aquaporin membranes for osmotic membrane bioreactors: Membrane performance and contaminant removal, Bioresour. Technol. 249 (2018) 62–68. doi:10.1016/J.BIORTECH.2017.09.170.

[26] Y. Zhao, C. Qiu, X. Li, A. Vararattanavech, W. Shen, J. Torres, C. Hélix-Nielsen, R. Wang, X. Hu, A.G. Fane, C.Y. Tang, Synthesis of robust and high-performance aquaporin-based biomimetic membranes by interfacial polymerization-membrane preparation and RO performance characterization, J. Memb. Sci. 423–424 (2012) 422–428. doi:10.1016/J.MEMSCI.2012.08.039.

[27] S. Qi, R. Wang, G.K.M. Chaitra, J. Torres, X. Hu, A.G. Fane, Aquaporin-based biomimetic reverse

osmosis membranes: Stability and long term performance, J. Memb. Sci. 508 (2016) 94–103. doi:10.1016/J.MEMSCI.2016.02.013.

[28] H. Wang, T.-S. Chung, Y.W. Tong, K. Jeyaseelan, A. Armugam, Z. Chen, M. Hong, W. Meier, Highly Permeable and Selective Pore-Spanning Biomimetic Membrane Embedded with Aquaporin Z, Small. 8 (2012) 1185–1190. doi:10.1002/smll.201102120.

[29] O. Kedem, A. Katchalsky, Permeability of composite membranes. Part 3.—Series array of elements, Trans. Faraday Soc. 59 (1963) 1941–1953. doi:10.1039/TF9635901941.

[30] C. Labbez, P. Fievet, A. Szymczyk, A. Vidonne, A. Foissy, J. Pagetti, Analysis of the salt retention of a titania membrane using the "DSPM" model: effect of pH, salt concentration and nature, J. Memb. Sci. 208 (2002) 315–329. doi:10.1016/S0376-7388(02)00310-1.

[31] X. Lu, C. Boo, J. Ma, M. Elimelech, Bidirectional diffusion of ammonium and sodium cations in forward osmosis: Role of membrane active layer surface chemistry and charge, Environ. Sci. Technol. 48 (2014) 14369–14376. doi:10.1021/es504162v.

[32] N.T. Hancock, T.Y. Cath, Solute Coupled Diffusion in Osmotically Driven Membrane Processes, Environ. Sci. Technol. 43 (2009) 6769–6775. doi:10.1021/es901132x.

[33] A. Schaefer, A.G. Fane, T. Waite, Nanofiltration : Principles and Applications / Ed. de A.I. Schäfer, A.G. Fane, T.D. Waite ; pról. de Robert J. Petersen., 2018.

[34] A. Achilli, T.Y. Cath, A.E. Childress, Selection of inorganic-based draw solutions for forward osmosis applications, J. Memb. Sci. 364 (2010) 233–241. doi:10.1016/J.MEMSCI.2010.08.010.

[35] S. Zhang, K.Y. Wang, T.-S. Chung, H. Chen, Y.C. Jean, G. Amy, Well-constructed cellulose acetate membranes for forward osmosis: Minimized internal concentration polarization with an ultra-thin selective layer, J. Memb. Sci. 360 (2010) 522–535. doi:10.1016/J.MEMSCI.2010.05.056.

[36] C. Boo, S. Lee, M. Elimelech, Z. Meng, S. Hong, Colloidal fouling in forward osmosis: Role of reverse salt diffusion, J. Memb. Sci. 390–391 (2012) 277–284. doi:10.1016/j.memsci.2011.12.001.

[37] G. Han, T.-S. Chung, M. Toriida, S. Tamai, Thin-film composite forward osmosis membranes with novel hydrophilic supports for desalination, J. Memb. Sci. 423–424 (2012) 543–555. doi:10.1016/J.MEMSCI.2012.09.005.

[38] P.H.H. Duong, T.-S. Chung, Application of thin film composite membranes with forward osmosis technology for the separation of emulsified oil–water, J. Memb. Sci. 452 (2014) 117–126.

doi:10.1016/J.MEMSCI.2013.10.030.

[39] M. Xie, W.E. Price, L.D. Nghiem, M. Elimelech, Effects of feed and draw solution temperature and transmembrane temperature difference on the rejection of trace organic contaminants by forward osmosis, J. Memb. Sci. 438 (2013) 57–64. doi:10.1016/J.MEMSCI.2013.03.031.

[40] N. Widjojo, T.-S. Chung, M. Weber, C. Maletzko, V. Warzelhan, A sulfonated polyphenylenesulfone (sPPSU) as the supporting substrate in thin film composite (TFC) membranes with enhanced performance for forward osmosis (FO), Chem. Eng. J. 220 (2013) 15–23. doi:10.1016/J.CEJ.2013.01.007.

[41] M. Tian, C. Qiu, Y. Liao, S. Chou, R. Wang, Preparation of polyamide thin film composite forward osmosis membranes using electrospun polyvinylidene fluoride (PVDF) nanofibers as substrates, Sep. Purif. Technol. 118 (2013) 727–736. doi:10.1016/J.SEPPUR.2013.08.021.

[42] J. Wei, C. Qiu, C.Y. Tang, R. Wang, A.G. Fane, Synthesis and characterization of flat-sheet thin film composite forward osmosis membranes, J. Memb. Sci. 372 (2011) 292–302. doi:10.1016/j.memsci.2011.02.013.

[43] Danish Standard, Water Study. Determination of ammonium nitrogen, (1975) DS 224: 1975.

[44] Danish Standards, Dansk Standard, (1985) DS/EN ISO 291:1985.

[45] A.K.H. D'Haese, I. De Leersnyder, P. Vermeir, A.R.D. Verliefde, On negative rejection of uncharged organic solutes in forward osmosis, J. Memb. Sci. 548 (2018) 22–31. doi:10.1016/J.MEMSCI.2017.11.002.

Supplementary Information

Changes in the feed concentrations of ammonium, chloride, and phosphate in FO experiments at pH = 10 are shown in Fig. S1. The figure shows water recovery steadily increasing along with the chloride feed concentration; however, ammonium concentration remains almost constant due to poor rejection.

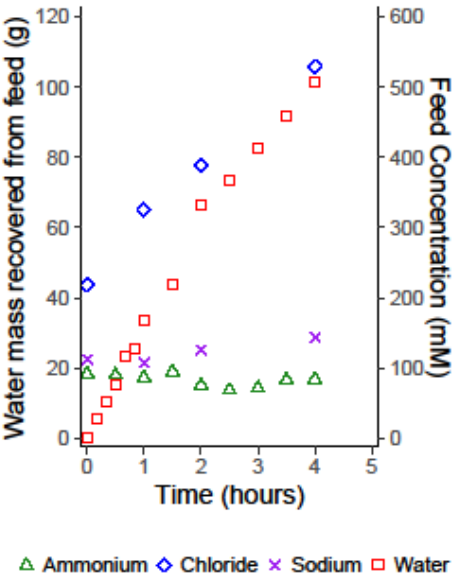

Fig. S1. Changes in water volume and feed concentration in experiments conducted at pH 10 using 25g L^{-1} NaCl draw solution.

The ratio between ammoniacal nitrogen and chloride flux was calculated as the slope of the linear regression between forward ammoniacal nitrogen flux and reverse chloride flux and plotted against pH in Fig. S2.

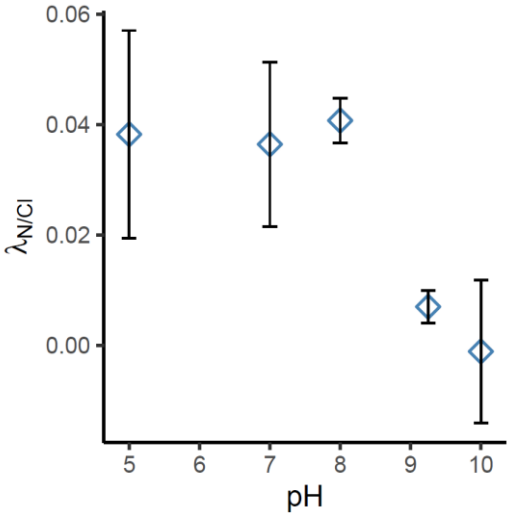

Fig. S2. Ratio between forward ammoniacal nitrogen and reverse chloride flux, $\lambda_{N/Cl}$, plotted against pH.

The plot shows that there is a great surplus of chloride ion transport relative to ammoniacal nitrogen transport. Chloride ions are transported from draw to feed and is not facilitating ammonium transport from feed to draw.

.

Table S1 shows the linear regression of the ammoniacal forward nitrogen flux versus sodium reverse flux at each pH.

Table S1
Linear regression model and correlation fit for data in Fig. 5a.

pH	Slope	Standard deviation	Intercept ($\times 10^{-5}$ mmol m^{-2} s^{-1})	R^2
5	0.219	0.014	0.6	0.342
7	0.265	0.050	1	0.934
8	0.152	0.058	3	0.777
9.25	-0.091	0.066	8	0.487
10	-0.024	0.014	6	0.604

Table S2 shows the hydrated radii (pm) and diffusivities (cm^2 s^{-1}) of multiple ions.

Table S2
Molecular weights, hydrated radii, and diffusivities of common solutes in digester centrate [21].

Ion	Molecular weight (g mol^{-1})	Hydrated radius (pm)	Diffusivity ($\times 10^{-5}$ cm^2 s^{-1})
Na^+	22.99	360	1.33
K^+	39.09	330	1.96
Mg^{2+}	24.31	430	1.41
Ca^{2+}	40.08	410	0.79
Cl^-	35.45	330	2.03
NH_4^+	18.04	330	1.96
NH_3	17.03	180	-

Highlights

- A bench-scale forward osmosis setup was used to concentrate digester centrate.
- Ammoniacal nitrogen flux was determined at varying pH and reverse salt flux.
- Reverse sodium flux was found to facilitate ammoniacal nitrogen flux at pH < 9.
- Ammoniacal nitrogen flux increased with feed pH, leading to no rejection at pH 10.
- It is recommended to operate at pH < 8 and use a draw solute with low reverse flux.